LETTERS

Experimental observation of the quantum Hall effect and Berry's phase in graphene

Yuanbo Zhang[1], Yan-Wen Tan[1], Horst L. Stormer[1,2] & Philip Kim[1]

When electrons are confined in two-dimensional materials, quantum-mechanically enhanced transport phenomena such as the quantum Hall effect can be observed. Graphene, consisting of an isolated single atomic layer of graphite, is an ideal realization of such a two-dimensional system. However, its behaviour is expected to differ markedly from the well-studied case of quantum wells in conventional semiconductor interfaces. This difference arises from the unique electronic properties of graphene, which exhibits electron–hole degeneracy and vanishing carrier mass near the point of charge neutrality[1,2]. Indeed, a distinctive half-integer quantum Hall effect has been predicted[3–5] theoretically, as has the existence of a non-zero Berry's phase (a geometric quantum phase) of the electron wavefunction—a consequence of the exceptional topology of the graphene band structure[6,7]. Recent advances in micromechanical extraction and fabrication techniques for graphite structures[8–12] now permit such exotic two-dimensional electron systems to be probed experimentally. Here we report an experimental investigation of magneto-transport in a high-mobility single layer of graphene. Adjusting the chemical potential with the use of the electric field effect, we observe an unusual half-integer quantum Hall effect for both electron and hole carriers in graphene. The relevance of Berry's phase to these experiments is confirmed by magneto-oscillations. In addition to their purely scientific interest, these unusual quantum transport phenomena may lead to new applications in carbon-based electronic and magneto-electronic devices.

The low-energy band structure of graphene can be approximated as cones located at two inequivalent Brillouin zone corners (Fig. 1a, left inset). In these cones, the two-dimensional (2D) energy dispersion relation is linear and the electron dynamics can be treated as 'relativistic', in which the Fermi velocity v_F of the graphene substitutes for the speed of light. In particular, at the apex of the cones (termed the Dirac point), electrons and holes (particles and antiparticles) are degenerate. Landau-level (LL) formation for electrons in this system under a perpendicular magnetic field, B, has been studied theoretically using an analogy to 2 + 1-dimensional quantum electrodynamics[2,3], in which the Landau level energy is given by

$$E_n = \mathrm{sgn}(n)\sqrt{2e\hbar v_F^2|n|B} \qquad (1)$$

Here e and $\hbar = h/2\pi$ are electron charge and Planck's constant divided by 2π, and the integer n represents an electron-like ($n > 0$) or a hole-like ($n < 0$) LL index. Crucially, a single LL with $n = 0$ and $E_0 = 0$ also occurs. When only low-lying LLs ($|n| < 10^4$ for $B = 10$ T) are occupied, the separation of E_n is much larger than the Zeeman spin splitting, so each LL has a degeneracy $g_s = 4$, accounting for spin degeneracy and sublattice degeneracy. Previous studies of mesoscopic graphite samples consisting of a few layers of graphene exhibited magneto-oscillations associated with the LL formation by electron-like and hole-like carriers tuned by the electric field effect[8,9,11]. However, the quantum Hall effect (QHE) was not observed in these samples, possibly as a result of their low mobility and/or the residual three-dimensional nature of the specimens.

The high-mobility graphene samples used in our experiments were extracted from Kish graphite (Toshiba Ceramics) on degenerately doped Si wafers with a 300-nm SiO_2 coating layer, by using micromechanical manipulation similar to that described in ref. 8.

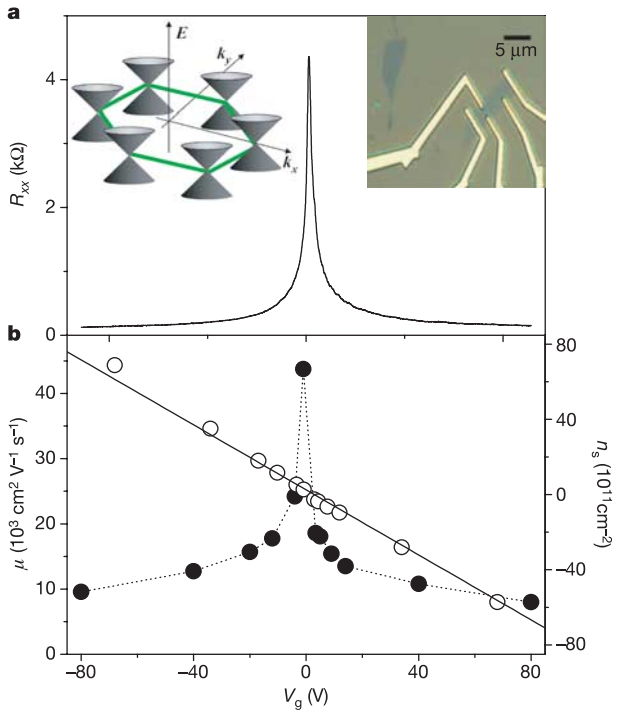

Figure 1 | Resistance, carrier density, and mobility of graphene measured at 1.7 K at different gate voltages. a, Changes in resistance as a function of gate voltage in a graphene device shown in the optical microscope image in the right inset. The position of the resistance peaks varies from device to device, but the peak values are always of the order of 4 kΩ, suggesting a potential quantum-mechanical origin. The left inset shows a schematic diagram of the low-energy dispersion relation near the Dirac points in the graphene Brillouin zone. Only two Dirac cones are nonequivalent to each other, producing a twofold valley degeneracy in the band structure. **b**, Charge carrier density (open circles) and mobility (filled circles) of graphene as a function of gate voltage. The solid line corresponds to the estimated charge induced by the gate voltage, $n_s = C_g V_g/e$, assuming a gate capacitance C_g of 115 aF μm^{-2} obtained from geometrical considerations.

[1]Department of Physics, [2]Department of Applied Physics and Applied Mathematics, Columbia University, New York, New York 10027, USA.

Interference-induced colour shifts, cross-correlated with an atomic force microscopy profile, allow us to identify the number of deposited graphene layers from optical images of the samples (Supplementary Information). After a suitable graphene sample has been selected, electron beam lithography followed by thermally evaporated Au/Cr (30 nm and 5 nm, respectively) defines multiple electrodes for transport measurement (Fig. 1a, right inset). With the use of a Hall-bar-type electrode configuration, the magnetoresistance R_{xx} and Hall resistance R_{xy} are measured. Applying a gate voltage, V_g, to the Si substrate controls the charge density in the graphene samples.

Figure 1a shows the gate modulation of R_{xx} at zero magnetic field in a typical graphene device whose lateral size is $\sim$3 μm. Whereas R_{xx} remains in the $\sim$100-Ω range at high carrier density, a sharp peak at $\sim$4 kΩ is observed at $V_g \approx 0$. Although different samples show slightly different peak values and peak positions, similar behaviours were observed in three other graphene samples that we measured. The existence of this sharp peak is consistent with the reduced carrier density as E_F approaches the Dirac point of grapheme, at which the density of states vanishes. Thus, the gate voltage corresponding to the charge-neutral Dirac point, V_{Dirac}, can be determined from this peak position. A separate Hall measurement provides a measure for the sheet carrier density, n_s, and for the mobility, μ, of the sample, as shown in Fig. 1b, assuming a simple Drude model. The sign of n_s changes at $V_g = V_{Dirac}$, indicating that E_F does indeed cross the charge-neutral point. Mobilities are higher than $10^4\,cm^2\,V^{-1}\,s^{-1}$ for the entire gate voltage range, considerably exceeding the quality of graphene samples studied previously[8,9].

The exceptionally high-mobility graphene samples allow us to investigate transport phenomena in the extreme magnetic quantum limit, such as the QHE. Figure 2a shows R_{xy} and R_{xx} for the sample of Fig. 1 as a function of magnetic field B at a fixed gate voltage $V_g > V_{Dirac}$. The overall positive R_{xy} indicates that the contribution is mainly from electrons. At high magnetic field, $R_{xy}(B)$ exhibits plateaux and R_{xx} is vanishing, which are the hallmark of the QHE. At least two well-defined plateaux with values $(2e^2/h)^{-1}$ and $(6e^2/h)^{-1}$, followed by a developing $(10e^2/h)^{-1}$ plateau, are observed before the QHE features transform into Shubnikov de Haas (SdH) oscillations at lower magnetic field. The quantization of R_{xy} for these first two plateaux is better than 1 part in 10^4, precise within the instrumental uncertainty. We observed the equivalent QHE features for holes with negative R_{xy} values (Fig. 2a, inset). Alternatively, we can probe the QHE in both electrons and holes by fixing the magnetic field and changing V_g across the Dirac point. In this case, as V_g increases, first holes ($V_g < V_{Dirac}$) and later electrons ($V_g > V_{Dirac}$) fill successive Landau levels and exhibit the QHE. This yields an antisymmetric (symmetric) pattern of R_{xy} (R_{xx}) in Fig. 2b, with R_{xy} quantization in accordance with

$$R_{xy}^{-1} = \pm g_s(n+1/2)e^2/h \qquad (2)$$

where n is a non-negative integer and ± stands for electrons and holes, respectively. This quantization condition can be translated to the quantized filling factor $\nu = \pm g_s(n+1/2)$ in the usual QHE language. In addition, there is an oscillatory structure developed near the Dirac point. Although this structure is reproducible for any given sample, its shape varies from device to device, suggesting potentially mesoscopic effects depending on the details of the sample geometry[13]. Although the QHE has been observed in many 2D

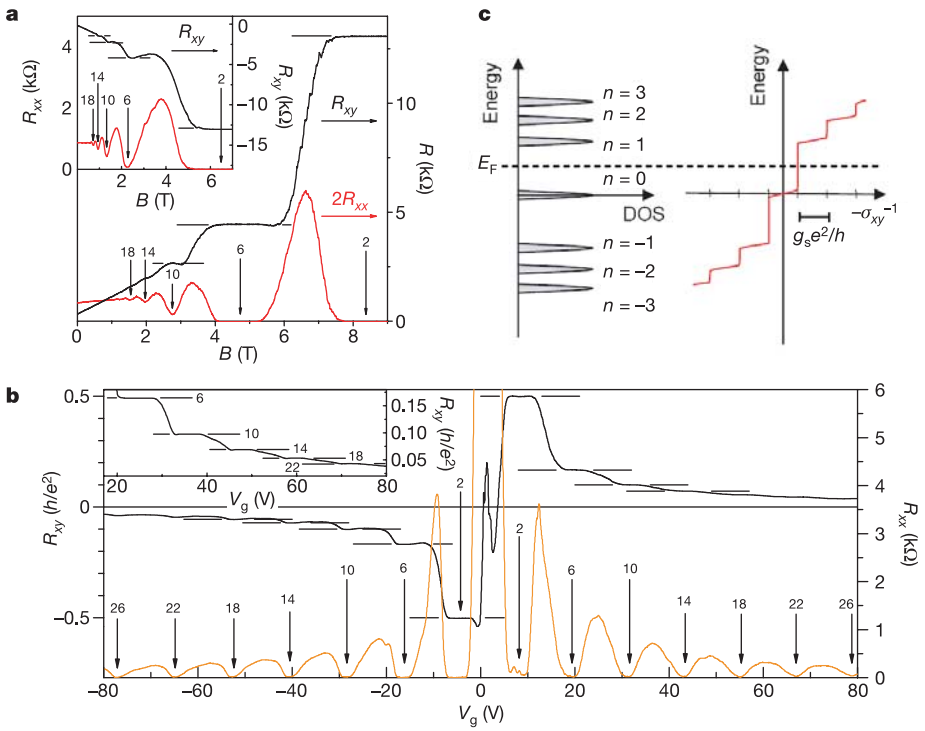

Figure 2 | Quantized magnetoresistance and Hall resistance of a graphene device. **a**, Hall resistance (black) and magnetoresistance (red) measured in the device in Fig. 1 at $T = 30$ mK and $V_g = 15$ V. The vertical arrows and the numbers on them indicate the values of B and the corresponding filling factor ν of the quantum Hall states. The horizontal lines correspond to $h/e^2\nu$ values. The QHE in the electron gas is shown by at least two quantized plateaux in R_{xy}, with vanishing R_{xx} in the corresponding magnetic field regime. The inset shows the QHE for a hole gas at $V_g = -4$ V, measured at 1.6 K. The quantized plateau for filling factor $\nu = 2$ is well defined, and the second and third plateaux with $\nu = 6$ and $\nu = 10$ are also resolved. **b**, Hall resistance (black) and magnetoresistance (orange) as a function of gate voltage at fixed magnetic field $B = 9$ T, measured at 1.6 K. The same convention as in **a** is used here. The upper inset shows a detailed view of high-filling-factor plateaux measured at 30 mK. **c**, A schematic diagram of the Landau level density of states (DOS) and corresponding quantum Hall conductance (σ_{xy}) as a function of energy. Note that, in the quantum Hall states, $\sigma_{xy} = -R_{xy}^{-1}$. The LL index n is shown next to the DOS peak. In our experiment the Fermi energy E_F can be adjusted by the gate voltage, and R_{xy}^{-1} changes by an amount $g_s e^2/h$ as E_F crosses a LL.

systems, the QHE observed in graphene is distinctively different those 'conventional' QHEs because the quantization condition (equation (2)) is shifted by a half-integer. These unusual quantization conditions are a result of the topologically exceptional electronic structure of grapheme, which we discuss below.

The sequence of half-integer multiples of quantum Hall plateaux has been predicted by several theories that combine 'relativistic' Landau levels with the particle–hole symmetry of graphene[3–5]. This can be easily understood from the calculated LL spectrum (equation (1)) as shown in Fig. 2c. Here we plot the density of states of the g_s-fold degenerate (spin and sublattice) of LLs and the corresponding Hall conductance ($\sigma_{xy} = -R_{xy}^{-1}$, for $R_{xx} \to 0$) in the quantum Hall regime as a function of energy. σ_{xy} exhibits QHE plateaux when E_F (tuned by V_g) falls between LLs, and jumps by an amount of $g_s e^2/h$ when E_F crosses a LL. Time-reversal invariance guarantees particle–hole symmetry; σ_{xy} is therefore an odd function in energy across the Dirac point[2]. However, in graphene, the $n = 0$ LL is robust—that is, $E_0 = 0$ regardless of the magnetic field—provided that the sublattice symmetry is preserved[2]. Thus, the first plateau of R_{xy}^{-1} for electron and hole is situated exactly at $\pm g_s e^2/2h$. As E_F crosses the next electron (hole) LL, R_{xy}^{-1} increases (decreases) by an amount $g_s e^2/h$, which yields the quantization condition in equation (2).

As noted by several workers, a consequence of the combination of time-reversal symmetry with the novel Dirac point structure can be viewed in terms of Berry's phase arising from the band degeneracy point[7,14]. A direct implication of Berry's phase in graphene is discussed in the context of the quantum phase of a spin-1/2 pseudo-spinor that describes the sublattice symmetry[6,15]. This phase is already implicit in the half-integer-shifted quantization rules of the QHE. It can further be probed in the magnetic field regime, in which a semi-classical magneto-oscillation description holds[16,17]:

$$\Delta R_{xx} = R(B,T)\cos[2\pi(B_F/B + 1/2 + \beta)] \qquad (3)$$

Here $R(B,T)$ is the SdH oscillation amplitude, B_F is the frequency of the SdH oscillation in $1/B$, and β is the associated Berry's phase, in the range $0 < \beta < 1$. Berry's phase $\beta = 0$ (or, equivalently, $\beta = 1$) corresponds to the trivial case. A deviation from this value is indicative of new physics with $\beta = 1/2$, implying the existence of Dirac particles[7]. Experimentally, this phase shift in the semi-classical regime can be obtained from an analysis of the SdH fan diagram, in which the sequence of values of $1/B_n$ of the nth minimum in R_{xx} are plotted against their index n (Fig. 3b). The intercept of linear fit to the data with the n-index axis yields Berry's phase, modulo an integer. The resulting β is very close to 0.5 (Fig. 3b, upper inset), providing further manifestation of the existence of a non-zero Berry's phase in graphene and the presence of Dirac particles. Such a non-zero Berry's phase was not observed in the previous few-layer graphite specimens[8,11,18], although there have been claims of hints of a phase shift in earlier measurements on bulk graphite[17]. Our data for graphene provide indisputable evidence for such an effect in a solid-state system.

The non-zero Berry's phase observed in the SdH fan diagram is related to the vanishing mass at the Dirac point. We can extract this effective carrier mass m_c from the temperature dependence of the well-developed SdH oscillations at low B field (Fig. 3a, left inset) by using the standard SdH formalism[19]. Indeed, the analysis at different gate voltages yields a strong suppression of m_c near the Dirac point. Whereas the high-density ($n_s \sim 5 \times 10^{12}\,\mathrm{cm}^{-2}$) carrier gas shows $m_c \sim 0.04 m_e$, the mass drops to $m_c \sim 0.007 m_e$ near the Dirac point ($n_s \sim 2 \times 10^{11}\,\mathrm{cm}^{-2}$), where m_e is the mass of the free electron. Overall, the observed gate voltage-dependent effective mass can be fitted to a fictitious 'relativistic' mass: $m_c = E_F/v_F^2 = \sqrt{(\pi\hbar^2 n_s/v_F^2)}$ by using v_F as the only fitting parameter (Fig. 3a, right inset). In accordance with the Berry's phase argument, this procedure extrapolates to a vanishing mass at the Dirac point.

Thus, we have experimentally discovered an unusual QHE in high-quality graphene samples. In contrast with conventional 2D systems, in graphene the observed quantization condition is described by half-integer rather than integer values. The measured phase shift in magneto-oscillation can be attributed to the peculiar topology of the graphene band structure with a linear dispersion relation and vanishing mass near the Dirac point, which can be described in terms of fictitious 'relativistic' carriers. The unique behaviour of electrons in this newly discovered 2 + 1-dimensional quantum electrodynamics system not only opens up many interesting questions in mesoscopic transport in electronic systems with non-zero Berry's phase but may also provide the basis for new applications in carbon-based electric and magnetic field-effect devices, such as ballistic metallic/semiconducting graphene ribbon devices[9] and electric field effective spin transport devices using a spin-polarized edge state[20].

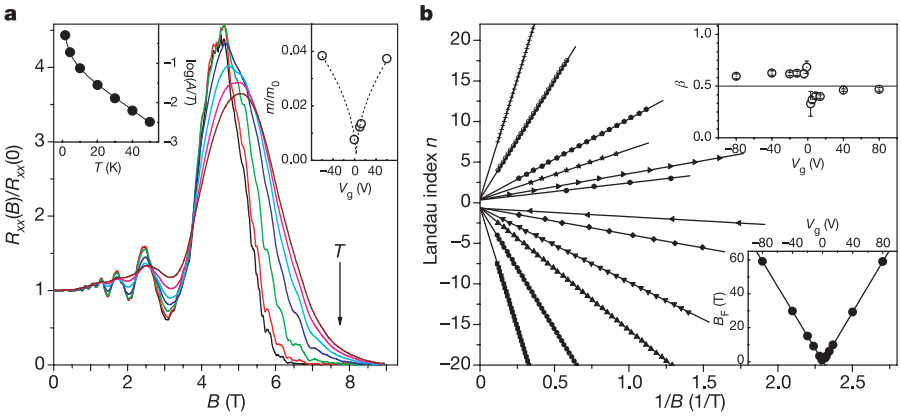

Figure 3 | Temperature dependence and gate-voltage dependence of the SdH oscillations in graphene. a, Temperature dependence of the SdH oscillations at $V_g = -2.5$ V. Each curve represents $R_{xx}(B)$ normalized to $R_{xx}(0)$ at a fixed temperature. The curves are in order of decreasing temperature, starting from the top, as indicated by the vertical arrow. The corresponding temperatures are shown in the left inset, which represents the SdH oscillation amplitude A divided by temperature measured at a fixed magnetic field. The standard SdH fit yields the effective mass. The right inset is a plot of the effective mass obtained at different gate voltages. The broken line is a fit to the single-parameter model described in the text, which yields $v_F = 1.1 \times 10^6\,\mathrm{m\,s}^{-1}$, in reasonable agreement with published values. **b**, A fan diagram for SdH oscillations at different gate voltages. The location of $1/B$ for the nth minimum (maximum) of R_{xx}, counting from $B = B_F$, plotted against n ($n + 1/2$). The lines correspond to a linear fit, in which the slope (lower inset) indicates B_F and the n-axis intercept (upper inset) provides a direct probe of Berry's phase in the magneto-oscillation in graphene. The error bars indicate the standard deviation of fitting errors.

Received 18 July; accepted 12 September 2005.

1. Semenoff, G. W. Condensed-matter simulation of a three-dimensional anomaly. *Phys. Rev. Lett.* **53,** 2449–2452 (1984).
2. Haldane, F. D. M. Model for a quantum hall effect without Landau levels: condensed-matter realization of the "parity anomaly". *Phys. Rev. Lett.* **61,** 2015–2018 (1988).
3. Zheng, Y. & Ando, T. Hall conductivity of a two-dimensional graphite system. *Phys. Rev. B* **65,** 245420 (2002).
4. Gusynin, V. P. & Sharapov, S. G. Unconventional integer quantum Hall effect in graphene. Preprint at ⟨http://xxx.lanl.gov/abs/cond-mat/0506575⟩ (2005).
5. Peres, N. M. R., Guinea, F. & Neto, A. H. C. Electronic properties of two-dimensional carbon. Preprint at ⟨http://xxx.lanl.gov/abs/cond-mat/0506709⟩ (2005).
6. Ando, T., Nakaishi, T. & Saito, R. Berry's phase and absence of back scattering in carbon nanotubes. *J. Phys. Soc. Jpn.* **67,** 2857–2862 (1998).
7. Mikitik, G. P. & Sharlai, Y. V. Manifestation of Berry's phase in metal physics. *Phys. Rev. Lett.* **82,** 2147–2150 (1999).
8. Novoselov, K. S. *et al.* Electric field effect in atomically thin carbon films. *Science* **306,** 666–669 (2004).
9. Berger, C. *et al.* Ultrathin epitaxial graphite: 2D electron gas properties and a route toward graphene-based nanoelectronics. *J. Phys. Chem. B* **108,** 19912–19916 (2004).
10. Zhang, Y., Small, J. P., Pontius, W. V. & Kim, P. Fabrication and electric-field-dependent transport measurements of mesoscopic graphite devices. *Appl. Phys. Lett.* **86,** 073104 (2005).
11. Zhang, Y., Small, J. P., Amori, E. S. & Kim, P. Electric field modulation of galvanomagnetic properties of mesoscopic graphite. *Phys. Rev. Lett.* **94,** 176803 (2005).
12. Bunch, J. S., Yaish, Y., Brink, M., Bolotin, K. & McEuen, P. L. Coulomb oscillations and Hall effect in quasi-2D graphite quantum dots. *Nano Lett.* **5,** 287–290 (2005).
13. Roukes, M. L., Scherer, A. & Van der Gaag, B. P. Are transport anomalies in 'electron waveguides' classical? *Phys. Rev. Lett.* **64,** 1154–1157 (1990).
14. Fang, Z. *et al.* The anomalous Hall effect and magnetic monopoles in momentum space. *Science* **302,** 92–95 (2003).
15. McEuen, P. L., Bockrath, M., Cobden, D. H., Yoon, Y. & Louie, S. G. Disorder, pseudospins, and backscattering in carbon nanotubes. *Phys. Rev. Lett.* **83,** 5098–5101 (1999).
16. Sharapov, S. G., Gusynin, V. P. & Beck, H. Magnetic oscillations in planar systems with the Dirac-like spectrum of quasiparticle excitations. *Phys. Rev. B* **69,** 075104 (2004).
17. Luk'yanchuk, I. A. & Kopelevich, Y. Phase analysis of quantum oscillations in graphite. *Phys. Rev. Lett.* **93,** 166402 (2004).
18. Morozov, S. V. *et al.* Two dimensional electron and hole gases at the surface of graphite. Preprint at ⟨http://xxx.lanl.gov/abs/cond-mat/0505319⟩ (2005).
19. Shoenberg, D. *Magnetic Oscillation in Metals* (Cambridge Univ. Press, Cambridge, 1984).
20. Kane, C. L & Mele, E. J. Quantum spin Hall effect in graphene. Preprint at ⟨http://xxx.lanl.gov/abs/cond-mat/0411737⟩ (2005).

Supplementary Information is linked to the online version of the paper at www.nature.com/nature.

Acknowledgements We thank I. Aleiner, A. Millis, T. F. Heinz, A. Mitra, J. Small and A. Geim for discussions. This research was supported by the NSF Nanoscale Science and Engineering Center at Columbia University, New York State Office of Science (NYSTAR) and the Department of Energy (DOE).

Author Information Reprints and permissions information is available at npg.nature.com/reprintsandpermissions. The authors declare no competing financial interests. Correspondence and requests for materials should be addressed to P.K. (pkim@phys.columbia.edu).